Global Optimization of Plug-In Hybrid Vehicle Design and Allocation to Minimize Life Cycle Greenhouse Gas Emissions

Ching-Shin Norman Shiau
Postdoctoral Research Fellow, Mechanical Engineering
Carnegie Mellon University,
Pittsburgh, PA 15213
e-mail: cshiau@andrew.cmu.edu

Jeremy J. Michalek[1]
Associate Professor, Mechanical Engineering
Engineering and Public Policy,
Carnegie Mellon University,
Pittsburgh, PA 15213
e-mail: jmichalek@cmu.edu

We pose a reformulated model for optimal design and allocation of conventional (CV), hybrid electric (HEV), and plug-in hybrid electric (PHEV) vehicles to obtain global solutions that minimize life cycle greenhouse gas (GHG) emissions of the fleet. The reformulation is a twice-differentiable, factorable, nonconvex mixed-integer nonlinear programming (MINLP) model that can be solved globally using a convexification-based branch-and-reduce algorithm. We compare results to a randomized multistart local-search approach for the original formulation and find that local-search algorithms locate global solutions in 59% of trials for the two-segment case and 18% of trials for the three-segment case. The results indicate that minimum GHG emissions are achieved with a mix of PHEVs sized for 25–45 miles of electric travel. Larger battery packs allow longer travel on electrical energy, but production and weight of underutilized batteries result in higher GHG emissions. Under the current average U.S. grid mix, PHEVs offer a nearly 50% reduction in life cycle GHG emissions relative to equivalent conventional vehicles and about 5% improvement over HEVs when driven on the standard urban driving cycle. Optimal allocation of different PHEVs to different drivers turns out to be of second order importance for minimizing net life cycle GHGs.
[DOI: 10.1115/1.4004538]

Keywords: global optimization, MINLP, plug-in hybrid electric vehicle, vehicle design, greenhouse gas emissions, global warming, transportation, life cycle assessment

1 Introduction

Plug-in hybrid electric vehicles (PHEVs) offer a potentially promising technology for addressing global warming in the U.S. transportation sector [1,2]. PHEVs are similar to ordinary hybrid electric vehicles (HEVs), except the PHEV carries a larger battery pack that can store energy from the electricity grid and propel the vehicle partly on electricity instead of gasoline [3]. Under the average mix of electricity sources in the U.S., vehicles can be driven with lower operation cost and fewer greenhouse gas (GHG) emissions when powered by electricity rather than by gasoline [4].

Shiau et al. [5] posed an optimization model for conventional, hybrid, and plug-in vehicle design and allocation of vehicles to drivers in order to minimize net life cycle cost, greenhouse gas emissions, and petroleum consumption. Like many optimization models posed in the mechanical design literature, the resulting formulation is difficult to solve globally, despite relatively small dimensionality, because of undesirable properties, including nonconvexity, nonsmoothness, a mixture of discrete and continuous variables, and integration in the objective function. While small numbers of discrete variables can be handled through exhaustive enumeration, if necessary, the resulting nonconvex nonlinear programming (NLP) subproblems still present a challenge. We pose a reformulation of the GHG minimization model presented in Ref. [5] that can be solved globally using deterministic methods that offer assurance of global solution quality.

There are three general approaches for solving nonconvex NLPs: (1) use a local NLP solver to find local solutions and invoke randomized multistart to seek global solutions [6]; (2) use a stochastic algorithm such as genetic algorithms or simulated annealing [7], or (3) use deterministic global optimization methods. Methods in group (1) and (2) are easy to implement, but they do not guarantee global solutions in finite time, and comparison of solutions across cases in sensitivity analysis is subject to uncertainty in attainment of global solutions in each sensitivity case. Methods in group (3) include gradient-based and derivative-free algorithms. Derivative-free deterministic global search algorithms that use partitioning, such as the divided rectangles method, perform well only in low dimensional spaces (<10 variables) and can perform poorly on equality-constrained problems [8]. In contrast, gradient-based global solvers, such as the branch and reduce optimization navigator (BARON), can produce global solutions for some significantly larger problems, but they require that objective and constraint functions be twice-differentiable, factorable algebraic functions so that valid convex underestimation functions can be automatically constructed to produce lower bounds in nodes of the branch and bound tree [9].

We pose a twice-differentiable, factorable, nonconvex mixed-integer nonlinear programming (MINLP) reformulation of the PHEV design and allocation problem that can be solved globally using BARON. In Sec. 2, we summarize the original model and pose our reformulation. In Sec. 3, we report solutions for minimum GHG emissions and compare the solution performance to a randomized multistart approach with a local NLP solver. We then conclude in Sec. 4.

2 Model

The model posed in Shiau et al. [5] partitions the population of drivers into a finite number of segments $i \in \{1, 2, \ldots n\}$, where each segment i contains all drivers who travel between s_{i-1} and s_i miles/day. The drivers in each segment i are assigned a vehicle defined by design variable vector x_i. The problem of minimizing daily life cycle GHG emissions from the fleet is written as

$$\begin{aligned} &\underset{\mathbf{x}_i, s_i \forall i \in \{1,\ldots,n\}}{\text{minimize}} \sum_{i=1}^{n} \left(\int_{s_{i-1}}^{s_i} f_{\mathrm{O}}(\mathbf{x}_i, s) f_{\mathrm{S}}(s) ds \right) \\ &\text{subject to } \mathbf{g}(\mathbf{x}_i) \le \mathbf{0}; \mathbf{h}(\mathbf{x}_i) = \mathbf{0}; \quad \forall i \in \{1, \ldots, n\} \\ &\qquad s_i \ge s_{i-1}; \quad \forall i \in \{1, \ldots, n\} \\ &\text{where } s_0 = 0; s_n = \infty \end{aligned} \tag{1}$$

where $f_{\mathrm{S}}(s)$ is the probability density function in the population of drivers over the daily driving distance s, $f_{\mathrm{O}}(\mathbf{x}_i,s)$ is the daily life cycle GHG emissions associated with vehicle $\mathbf{x}_i$ when driven s miles/day, and $\mathbf{g}$ and $\mathbf{h}$ are inequality and equality constraints, respectively, that ensure the design variables $\mathbf{x}_i$ define a feasible vehicle. The design variables for the conventional vehicle (CV) and the HEV are determined a priori, since their GHG implications per mile do not depend on the distance driven. In contrast, GHG emissions from PHEVs depend on the distance driven between charges, since PHEVs use gasoline if the vehicle is driven further than its all-electric range (AER). Data from the National Household Travel Survey (NHTS) [10] are used to

[1]Corresponding author.

Manuscript received June 15, 2010; final manuscript received June 24, 2011; published online August 22, 2011. Assoc. Editor: Steven J. Skerlos. A version of this article appeared first in the 2010 ASME IDETC conference.

estimate $f_S(s) = \lambda e^{-\lambda s}$, where $\lambda = 0.0296$, assuming one charge per day. The PHEV design variable vector x_i consists of x_1 = engine size (kW), x_2 = motor size (kW), x_3 = battery size (kWh), x_4 = battery swing (%). Following Shiau et al. [5], the vehicle-specific daily GHG emissions are calculated as

$$f_O(\mathbf{x}, s) = \left(\frac{s_E(\mathbf{x}, s)}{\eta_E(\mathbf{x})}\frac{v_E}{\eta_C} + \frac{s_G(\mathbf{x}, s)}{\eta_G(\mathbf{x})}v_G\right) + \left(\frac{\nu_{VEH}}{\theta_{VEH}(s)}\right) + \left(\frac{1000x_3\kappa v_{BAT}}{\theta_{BRPL}(\mathbf{x}, s)}\right) \quad (2)$$

where the three parenthetical terms represent emissions associated with operation, vehicle production, and battery production, respectively. Specifically, $v_E = 0.752$ kg-CO_2-eq/kWh, $v_G = 11.34$ kg-CO_2-eq/gal, $v_{VEH} = 8500$ kg-CO_2-eq/vehicle, and $v_{BAT} = 120$ kg-CO_2-eq/kWh are life cycle GHG emissions associated with electricity, gasoline, vehicle production, and battery production, respectively; η_E and η_G are the electrical and gasoline efficiency of the vehicle, respectively; $\eta_C = 88\%$ is the charging efficiency; $\theta_{VEH} = s_{LIFE}/s$ is the vehicle life in days, where $s_{LIFE} = 150{,}000$ miles; $\theta_{BRPL} = \min(\theta_{VEH}, \theta_{BAT})$ is the effective battery replacement life; $\theta_{BAT} = (1000x_3)\kappa r_{EOL}/(\alpha_{DRV}(\mu_{CD}s_E + \mu_{CS}s_G) + \alpha_{CHG}s_E(\eta_E\eta_B)^{-1})$ is the full battery life; $r_{EOL} = 20\%$ is the battery end-of-life criterion; $\alpha_{DRV} = 3.46 \times 10^{-5}$ and $\alpha_{CHG} = 1.72 \times 10^{-5}$ are the coefficients for relative energy capacity fade, based on degradation data; μ_{CD} and μ_{CS} are energy processed per mile (kWh/mile) in charge-depleting (CD) and charge-sustaining (CS) mode, respectively; $\eta_B = 95\%$ is the battery charging efficiency; $\kappa = 0.0216$ kWh/cell is the Li-ion battery energy capacity; and s_E and s_G are the distances traveled on electric power and gasoline power, respectively, so that $s_E = (s)(s \le s_{AER}) + (s_{AER})(s > s_{AER})$ and $s_G = (0)(s \le s_{AER}) + (s - s_{AER})(s > s_{AER})$ for a vehicle with an AER of $s_{AER} = \kappa(1000x_3)x_4\eta_E$ for PHEVs and $s_{AER} = 0$ for the CV and HEV cases. For the PHEV, the quantities η_E, η_G, μ_{CD}, μ_{CS}, t_{CD}, t_{CS}, and u_{CS} are calculated as functions of x using cubic metamodels of vehicle simulation data points, where t_{CD} and t_{CS} are the time to accelerate the vehicle from 0 to 60 mph in CD and CS mode (seconds), respectively, and u_{CS} is the level of charge maintenance in CS mode under an aggressive driving cycle (%). These quantities are calculated a priori for the CV and HEV cases, as appropriate. The constraints $\mathbf{g}$ consist of $t_{CD}(\mathbf{x}) \le 11$ s and $t_{CS}(\mathbf{x}) \le 11$ s, to ensure comparable vehicles, and $u_{CS} \ge 32\%$ to ensure sufficient engine size.

2.1 MINLP Reformulation. The original model formulation (Eq. (1)) involves integration, discrete decisions (vehicle type, not shown in Eq. (1)), and piecewise-smooth functions with derivative discontinuities due to AER and battery life. To solve the problem globally, we pose a factorable, algebraic nonconvex MINLP reformulation that can be solved using a convexification-based branch-and-reduce algorithm implemented in general algebraic modeling system (GAMS)/BARON [11]. First, the exponential distribution form for the NHTS data fit $f_S(s)$ allows the integral in Eq. (1) to be simplified in terms of two algebraic formulae: the cumulative density function F_S

$$F_S(s_i) = \int_0^{s_i} f_S(s)ds = 1 - e^{-\lambda s_i} \quad (3)$$

and the truncated expected value function F_E

$$F_E(s_i) = \int_0^{s_i} sf_S(s)ds = \frac{1}{\lambda} - e^{-\lambda s_i}\left(s_i + \frac{1}{\lambda}\right) \quad (4)$$

with these formulae the integral in Eq. (1) collapses to an explicit form. While it is also possible to eliminate the integral through numerical integration by discretizing the domain, the proposed formulation allows use of fewer discrete variables and achieves higher resolution. However, extension of the approach to minimize a discounted cost objective is nontrivial, since the integration variable appears in the discounting formula. We next introduce four sets of binary variables to convert the problem to a twice-differentiable MINLP. The first binary variable set t_{il} identifies the vehicle type $l \in \{1,2,..,L\}$ for each segment i, where $t_{il} \in \{0,1\}$ $\forall i,l$ and $\Sigma_l t_{il} = 1$ $\forall i$. Here, we consider three vehicle types $l \in \{1,2,3\}$ for CV, HEV, and PHEV, respectively, and write the objective function as a binary-weighted function $\sum_l (t_l)(f_l(\mathbf{x}_l, s))$.

The second binary variable set $z_{ij} \in \{0,1\}$ $\forall i,j$ handles one of the derivative discontinuities by identifying in which of three regions $j \in \{1,2,3\}$ on the s-axis each segment i is located, relative to s_{AER} ($\Sigma_j z_{ij} = 1$ $\forall i$).

(1) in region 1, $s_{AER} \le s_i \Rightarrow (z_{i1})(s_{AER}(\mathbf{x}_i) - s_{i\text{-}1}) \le 0$;
(2) in region 2, $s_{i-1} \le s_{AER} \le s_i \Rightarrow (z_{i2})(s_{i-1} - s_{AER}(\mathbf{x}_i)) \le 0$ and $(z_{i2})(s_{AER}(\mathbf{x}_i) - s_i) \le 0$;
(3) in region 3, $s_{AER} \ge s_i \Rightarrow (z_{i3})(s_i - s_{AER}(\mathbf{x}_i)) \le 0$.

While these bilinear functions, representing a disjunction, pose constraint qualification problems for NLP solvers that could be addressed through reformulation [12,13], our use of the solver BARON involves internal handling of these constraints through convexification and outer approximation with cutting planes, removing constraint qualification concerns. The third binary variable set q_{io} $o \in \{1,2,3\}$ and $\Sigma_o q_{io} = 1$ $\forall i$ identifies the relative conditions between battery life θ_{BAT} and vehicle life θ_{VEH}. The estimated battery life $s_{BAT} = s\theta_{BAT}$, in miles. If $s \le s_{AER}$, this expression reduces to $s_{BAT} = (1000x_3)\kappa r_{EOL}/(\alpha_{DRV}\mu_{CD} + \alpha_{CHG}(\eta_E\eta_B)^{-1})$. For $s > s_{AER}$, s_{BAT} is monotonically increasing and asymptotically approaches $s^{\infty}_{BAT} = (1000x_3\kappa r_{EOL})/(\alpha_{DRV}\mu_{CS})$ as $s \to \infty$. Given the shape of s_{BAT} ($s^{\infty}_{BAT} > s^{0}_{BAT}$), we can identify four possible relationships between s_{BAT} and vehicle life s_{LIFE}:

(a) if $s_{LIFE} \ge s^{\infty}_{BAT}$, then $s_{BAT} < s_{LIFE}$ $\forall s$;
(b) if $s^{\infty}_{BAT} > s_{LIFE} > s^{0}_{BAT}$, then s_{BAT} and s_{LIFE} intersect at $s_T = s_{LIFE}s_{AER}(\alpha_{DRV}(\mu_{CD} - \mu_{CS}) + \alpha_{CHG}(\eta_E\eta_B)^{-1})/(1000x_3\kappa r_{EOL} - \alpha_{DRV}\mu_{CS}s_{LIFE})$, $s_{BAT} < s_{LIFE}$ for $0 \le s < s_T$, and $s_{BAT} > s_{LIFE}$ for $s > s_T$
(c) if $s_{LIFE} = s\theta_{BAT}$, then $s_{BAT} = s_{LIFE}$ for $0 \le s \le s_{AER}$, and $s_{BAT} > s_{LIFE}$ for $s > s_T$ or
(d) if $s_{LIFE} < s\theta_{BAT}$, then $s_{BAT} > s_{LIFE}$ for all s.

The four conditions are illustrated in Fig. 1.

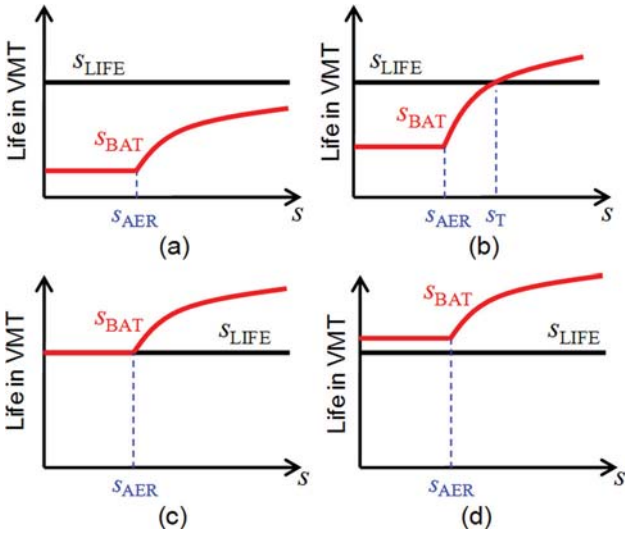

Fig. 1 Four conditions for the battery and vehicle VMT curves

Given $\theta_{BAT}(s)$, these conditions can be represented by three cases:

(1) in case 1 ($o=1$), $s^{\infty}{}_{BAT} \le s_{LIFE}$ ($\theta_{BAT} < \theta_{VEH}$) $\forall s \Rightarrow (q_{i1})(\theta_{BAT}(\infty) - \theta_{VEH}) \le 0$ and $\theta_{BRPL} = \theta_{BAT}$
(2) for case 2 ($o=2$), θ_{BAT} intersects θ_{VEH} at a point $s_T \Rightarrow (q_{i2})(\theta_{VEH} - \theta_{BAT}(\infty)) \le 0$ and $(q_{i2})(\theta_{BAT}(0) - \theta_{VEH}) \le 0$, so $\theta_{BRPL} = \theta_{BAT}$ for $s \le s_T$, $\theta_{BRPL} = \theta_{VEH}$ for $s \ge s_T$ and
(3) for case 3 ($o=3$), $s\theta_{BAT} \ge s_{LIFE}$ ($\theta_{BAT} \ge \theta_{VEH}$) $\forall s \Rightarrow (q_{i3})(\theta_{VEH} - \theta_{BAT}(0)) \le 0$ and $\theta_{BRPL} = \theta_{VEH}$.

The fourth binary variable set y_{ik} identifies in which region s_T lies when $q_{i2}=1$ ($o=2$). The three conditions $k \in \{1,2,3\}$ on the binary variable set y_{ik} are:

(1) in region 1 ($k=1$), $s_T(\mathbf{x}_i) \le s_{i-1} \Rightarrow (q_{i2})(y_{i1})(s_T(\mathbf{x}_i) - s_{i-1}) < 0$;
(2) in region 2 ($k=2$), $s_{i-1} \le s_T \le s_i \Rightarrow (q_{i2})(y_{i2})(s_{i-1} - s_T(\mathbf{x}_i)) \le 0$ and $(q_{i2})(y_{i2})(s_T(\mathbf{x}_i) - s_i) \le 0$; and
(3) in region 3 ($k=3$), $s_T(\mathbf{x}_i) \ge s_i \Rightarrow (q_{i2})(y_{i3})(s_i - s_T(\mathbf{x}_i)) \le 0$.

The combinations of j, k, and o result in 27 cases. For each segment i and for each of the cases $j \in \{1,2,3\}$ $k \in \{1,2,3\}$ $o \in \{1,2,3\}$, the integral in Eq. (1) reduces to a twice-differentiable closed form factorable algebraic expression $F_{ijko}(\mathbf{x}_{il}, s_{i-1}, s_i)$ using Eqs. (3) and (4). The population-weighted operation GHG emissions F_{OP} for segment i are

$$F_{OPi} = \int_{s_{i-1}}^{s_i} \left(\frac{s_E(\mathbf{x},s)}{\eta_E(\mathbf{x})} \frac{v_E}{\eta_C} + \frac{s_G(\mathbf{x},s)}{\eta_G(\mathbf{x})} v_G \right) f_S(s)ds = \sum_{j=1}^{3} z_{ij} F_{OPij}(\mathbf{x}_{il}, s_{i-1}, s_i)$$

where
$$F_{OPi1} = \frac{v_G}{\eta_{Gi}}(F_E(s_i) - F_E(s_{i-1})) + s_{AERi}\left(\frac{v_E}{\eta_{Ei}\eta_C} - \frac{v_G}{\eta_{Gi}}\right)(F_S(s_i) - F_S(s_{i-1}))$$
$$F_{OPi2} = \frac{v_E}{\eta_{Ei}\eta_C}(F_E(s_{AERi}) - F_E(s_{i-1})) + \frac{v_G}{\eta_{Gi}}(F_E(s_i) - F_E(s_{AERi})) + s_{AERi}\left(\frac{v_E}{\eta_{Ei}\eta_C} - \frac{v_G}{\eta_{Gi}}\right)(F_S(s_i) - F_S(s_{AERi}))$$
$$F_{OPi3} = \frac{v_E}{\eta_{Ei}\eta_C}(F_E(s_i) - F_E(s_{i-1})) \quad (5)$$

The population-weighted vehicle production GHG emissions F_{VEH} for segment i are

$$F_{VEHi} = \int_{s_{i-1}}^{s_i} \left(\frac{v_{VEH}}{\theta_{VEH}(s)} \right) f_S(s)ds = \frac{v_{VEH}}{s_{LIFE}}(F_E(s_i) - F_E(s_{i-1})) \quad (6)$$

and the population-weighted battery production GHG emissions F_{BAT} for vehicle i are

$$F_{BATi} = \int_{s_{i-1}}^{s_i} \left(\frac{1000 x_3 \kappa v_{BAT}}{\theta_{BRPL}(\mathbf{x},s)} \right) f_S(s)ds = \sum_{j=1}^{3}\sum_{k=1}^{3}\sum_{o=1}^{3} z_{ij} y_{ik} q_{io} F_{BATijko}(\mathbf{x}_{il}, s_{i-1}, s_i) \quad (7)$$

where the 27 $F_{BATijko}$ terms fall into six cases:

Case (1a): $\theta_{BRPL} = \theta_{BAT}$ and $s_{AERi} \le s_{i-1}$

$$F_{BAT1ai} = \frac{v_{BAT}}{r_{EOL}} \left[\alpha_{DRV} w_{CSi}(F_E(s_i) - F_E(s_{i-1})) + s_{AERi}\left(\alpha_{DRV} w_{CDi} + \alpha_{CHG}(\eta_{Ei}\eta_B)^{-1} - \alpha_{DRV} w_{CSi}\right) \times (F_S(s_i) - F_S(s_{i-1})) \right] \quad (8)$$

Case (1b): $\theta_{BRPL} = \theta_{BAT}$ and $s_{i-1} \le s_{AERi} \le s_i$

$$F_{BAT1bi} = \frac{v_{BAT}}{r_{EOL}} \left[\left(\alpha_{DRV}\mu_{CDi} + \alpha_{CHG}(\eta_{Ei}\eta_B)^{-1}\right) (F_E(s_{AERi}) - F_E(s_{i-1})) + \alpha_{DRV}\mu_{CS}(F_E(s_i) - F_E(s_{AERi})) + s_{AER}\left(\alpha_{DRV}\mu_{CDi} + \alpha_{CHG}(\eta_{Ei}\eta_B)^{-1} - \alpha_{DRV}\mu_{CSi}\right) (F_S(s_i) - F_S(s_{AERi})) \right] \quad (9)$$

Case (1c): $\theta_{BRPL} = \theta_{BAT}$ and $s_i \le s_{AERi}$

$$F_{BAT1c} = \frac{v_{BAT}}{r_{EOL}} \left(\alpha_{DRV}\mu_{CDi} + \alpha_{CHG}\eta_{Ei}^{-1}\right)(F_E(s_i) - F_E(s_{i-1})) \quad (10)$$

Case (2a): $\theta_{BRPL} = \{\theta_{BAT}, \theta_{VEH}\}$ and $s_{AERi} \le s_{i-1}$

$$F_{BAT2ai} = \frac{v_{BAT}}{r_{EOL}} \left[\alpha_{DRV}\mu_{CSi}(F_E(s_{Ti}) - F_E(s_{i-1})) + s_{AERi}\left(\alpha_{DRV}\mu_{CDi} + \alpha_{CHG}(\eta_{Ei}\eta_B)^{-1} - \alpha_{DRV}\mu_{CSi}\right) \times (F_S(s_{Ti}) - F_S(s_{i-1})) \right] + \frac{1000 x_3 \kappa v_{BAT}}{s_{LIFE}}(F_E(s_i) - F_E(s_{Ti})) \quad (11)$$

Case (2b): $\theta_{BRPL} = \{\theta_{BAT}, \theta_{VEH}\}$ and $s_{i-1} \le s_{AERi} \le s_i$

$$F_{BAT2bi} = \frac{v_{BAT}}{r_{EOL}} \left[\left(\alpha_{DRV}\mu_{CDi} + \alpha_{CHG}(\eta_{Ei}\eta_B)^{-1}\right) \times (F_E(s_{AERi}) - F_E(s_{i-1})) + \alpha_{DRV}\mu_{CSi}(F_E(s_{Ti}) - F_E(s_{AERi})) + s_{AER}\left(\alpha_{DRV}\mu_{CDi} + \alpha_{CHG}(\eta_{Ei}\eta_B)^{-1} - \alpha_{DRV}\mu_{CSi}\right) \times (F_S(s_{Ti}) - F_S(s_{AERi})) \right] + \frac{1000 x_3 \kappa v_{BAT}}{s_{LIFE}}(F_E(s_i) - F_E(s_{Ti})) \quad (12)$$

Case (3): $\theta_{BRPL} = \theta_{VEH}$

$$F_{BAT3i} = \frac{1000 x_3 \kappa v_{BAT}}{s_{LIFE}}(F_E(s_i) - F_E(s_{i-1})) \quad (13)$$

Table 1 presents the summary of the discrete conditions with corresponding θ_{BRPL} and the components in the total cost function. Among the $o=2$ cases, three are infeasible because $s_T > s_{AER}$ is required when s_T exists.

Table 1 Discrete conditions for the piecewise-smooth PHEV objective function

o		j		k		θ_{BRPL}	Total GHG function F_{ijko}
1	$s^{\infty}_{\text{BAT}i} \le s_{\text{LIFE}}$	1	$s_{\text{AER}i} \le s_{i-1}$				
		2	$s_{i-1} \le s_{\text{AER}i} \le s_i$			θ_{BAT}	$F_{i1k1}=F_{\text{VEH}i}+F_{\text{OP}i1}+F_{\text{BAT1a}i}$ $F_{i2k1}=F_{\text{VEH}i}+F_{\text{OP}i2}+F_{\text{BAT1b}i}$
		3	$s_i \le s_{\text{AER}i}$				$F_{i3k1}=F_{\text{VEH}i}+F_{\text{OP}i3}+F_{\text{BAT1c}i}$
2	$s^{0}_{\text{BAT}i} \le s_{\text{LIFE}} \le s^{\infty}_{\text{BAT}i}$	1	$s_{\text{AER}i} \le s_{i-1}$	1	$s_{\text{T}i} \le s_{i-1}$	θ_{VEH}	$F_{i112}=F_{\text{VEH}i}+F_{\text{OP}i1}+F_{\text{BAT3}i}$
				2	$s_{i-1} \le s_{\text{T}i} \le s_i$	$\{\theta_{\text{BAT}}, \theta_{\text{VEH}}\}$	$F_{i122}=F_{\text{VEH}i}+F_{\text{OP}i1}+F_{\text{BAT2a}i}$
				3	$s_i \le s_{\text{T}i}$	θ_{BAT}	$F_{i132}=F_{\text{VEH}i}+F_{\text{OP}i1}+F_{\text{BAT1a}i}$
		2	$s_{i-1} \le s_{\text{AER}i} \le s_i$	1	$s_{\text{T}i} \le s_{i-1}$	Infeasible	
				2	$s_{i-1} \le s_{\text{T}i} \le s_i$	$\{\theta_{\text{BAT}}, \theta_{\text{VEH}}\}$	$F_{i222}=F_{\text{VEH}i}+F_{\text{OP}i2}+F_{\text{BAT2b}i}$
				3	$s_i \le s_{\text{T}i}$	θ_{BAT}	$F_{i232}=F_{\text{VEH}i}+F_{\text{OP}i2}+F_{\text{BAT1b}i}$
		3	$s_i \le s_{\text{AER}i}$	1	$s_{\text{T}i} \le s_{i-1}$	Infeasible	
				2	$s_{i-1} \le s_{\text{T}i} \le s_i$	Infeasible	
				3	$s_i \le s_{\text{T}i}$	θ_{BAT}	$F_{i332}=F_{\text{VEH}i}+F_{\text{OP}i3}+F_{\text{BAT1c}i}$
3	$s^{0}_{\text{BAT}i} \ge s_{\text{LIFE}}$	1	$s_{\text{AER}i} \le s_{i-1}$				
		2	$s_{i-1} \le s_{\text{AER}i} \le s_i$			θ_{VEH}	$F_{i1k3}=F_{\text{VEH}i}+F_{\text{OP}i1}+F_{\text{BAT3}i}$ $F_{i2k3}=F_{\text{VEH}i}+F_{\text{OP}i2}+F_{\text{BAT3}i}$
		3	$s_i \le s_{\text{AER}i}$				$F_{i3k3}=F_{\text{VEH}i}+F_{\text{OP}i3}+F_{\text{BAT3}i}$

The complete MINLP formulation is

$$\underset{\substack{\mathbf{x}_{il},t_{il},z_{ij},y_{ik},q_{io},s_i \\ \forall i\in\{1,\ldots,n\} \\ \forall l,j,k,o\in\{1,2,3\}}}{\text{minimize}} \sum_{i=0}^{n}\sum_{l=1}^{3}\sum_{j=1}^{3}\sum_{k=1}^{3}\sum_{o=1}^{3} t_{il}z_{ij}y_{ik}q_{io}F_{ijko}(\mathbf{x}_{il}, s_{i-1}, s_i)$$

$$\text{subject to } \mathbf{x}_l^{\text{LB}} \le \mathbf{x}_{il} \le \mathbf{x}_l^{\text{UB}};\quad t_{\text{CD}i} \le 11;\quad t_{\text{CS}i} \le 11;\quad u_{\text{CS}i} \ge 32\%;$$

$$\sum_{l=1}^{3} t_{il} = 1;\quad \sum_{j=1}^{3} z_{ij} = 1;\quad \sum_{k=1}^{3} y_{ik} = 1;\quad \sum_{o=1}^{3} q_{io} = 1;\quad s_{i-1} \le s_i;$$

$$(z_{i1})(s_{\text{AER}i} - s_{i-1}) \le 0;\quad (z_{i2})(s_{i-1} - s_{\text{AER}i}) \le 0;$$

$$(z_{i2})(s_{\text{AER}i} - s_i) \le 0;\quad (z_{i3})(s_i - s_{\text{AER}i}) \le 0;$$

$$(q_{i1})\left(s^{\infty}_{\text{BAT}i} - s_{\text{LIFE}}\right) \le 0;\quad (q_{i2})\left(s^{0}_{\text{BAT}i} - s_{\text{LIFE}}\right) \le 0;$$

$$(q_{i2})\left(s_{\text{LIFE}} - s^{\infty}_{\text{BAT}i}\right) \le 0;\quad (q_{i3})\left(s_{\text{LIFE}} - s^{0}_{\text{BAT}i}\right) \le 0;$$

$$(q_{i2})(y_{i1})(s_{\text{T}i} - s_{i-1}) \le 0;\quad (q_{i2})(y_{i2})(s_{i-1} - s_{\text{T}i}) \le 0;$$

$$(q_{i2})(y_{i2})(s_{\text{T}i} - s_i) \le 0;\quad (q_{i2})(y_{i3})(s_i - s_{\text{T}i}) \le 0;$$

$$t_{il}, z_{ij}, y_{ik}, q_{io} \in \{0,1\};\quad s_i \in \mathbb{R};\quad \mathbf{x}_{il} \in \mathbb{R}^{p_l};$$

$$\forall i \in \{1,\ldots,n\};\quad \forall l,j,k,o \in \{1,2,3\}$$

$$\text{where } s_0 = 0;\quad s_n = \infty;\quad s_{\text{AER}i} = 10^3 t_{i3}\kappa[\mathbf{x}_{i3}]_3[\mathbf{x}_{i3}]_4\eta_{\text{E}i};$$

$$s^{0}_{\text{BAT}i} = \frac{10^3(\mathbf{x}_{i3})_3\kappa r_{\text{EOL}}}{\alpha_{\text{DRV}}\mu_{\text{CD}i} + \alpha_{\text{CHG}}\eta_{\text{E}i}{}^{-1}};\quad s^{\infty}_{\text{BAT}i} = \frac{10^3(\mathbf{x}_{i3})_3\kappa r_{\text{EOL}}}{\alpha_{\text{DRV}}\mu_{\text{CS}i}};$$

$$s_{\text{T}i} = \frac{s_{\text{LIFE}}s_{\text{AER}i}(\alpha_{\text{DRV}}(\mu_{\text{CD}i} - \mu_{\text{CS}i}) + \alpha_{\text{CHG}}\eta_{\text{E}i}{}^{-1})}{10^3(\mathbf{x}_{i3})_3\kappa r_{\text{EOL}} - \alpha_{\text{DRV}}\mu_{\text{CS}i}s_{\text{LIFE}}}$$

$$\eta_{\text{E}i} = \sum_l t_{il}f_{1l}(\mathbf{x}_{il});\quad \eta_{\text{G}i} = \sum_l t_{il}f_{2l}(\mathbf{x}_{il});$$

$$t_{\text{CD}i} = \sum_l t_{il}f_{3l}(\mathbf{x}_{il});\quad t_{\text{CS}i} = \sum_l t_{il}f_{4l}(\mathbf{x}_{il});$$

$$\mu_{\text{CD}i} = \sum_l t_{il}f_{5l}(\mathbf{x}_{il});\quad \mu_{\text{CS}i} = \sum_l t_{il}f_{6l}(\mathbf{x}_{il});$$

$$u_{\text{CS}i} = \sum_l t_{il}f_{7l}(\mathbf{x}_{il});$$

$$F_{ijko}(\mathbf{x}_{il}, s_{i-1}, s_i) = \int_{s_{i-1}}^{s_i} f_{\text{O}}(\mathbf{x}_i, s) f_{\text{S}}(s)\,ds \tag{14}$$

where the expression for F_{ijko} reduces to a twice-differentiable algebraic expression in each case, as defined in Table 1, $f_{11}=f_{12}=0$, $f_{21}=29.5$ mpg (CV), $f_{22}=60.1$ mpg (HEV), $f_{31}=f_{32}=0$, $f_{41}=f_{42}=11$ s, $f_{51}=f_{52}=f_{61}=f_{62}=0$, $f_{71}=f_{72}=1$, and $f_{m3}(\mathbf{x}_{il})$ are defined using cubic metamodels for PHEVs ($l=3$ and $t_{i3}=1$). The notation $[\mathbf{x}_{i3}]_3$ and $[\mathbf{x}_{i3}]_4$ refers to the design variable vector $\mathbf{x}$ for segment i vehicle type 3 (PHEV), vector element 3 and 4, respectively.

3 Results and Discussions

We consider three driver segment scenarios, $n=1$, 2, and 3, and solve the MINLP model (Eq. (14)) using BARON to obtain global solutions. The optimal vehicle type, design and allocation ranges for each case are summarized in Table 2. The first two data columns show the performance values of CV and HEV, for reference.

For the single-segment case, we found that a PHEV36 has the lowest lifecycle GHG emissions, where the notation PHEVx is used to designate a PHEV with a battery pack sized for x miles of all-electric travel. GHG emissions from the HEV scenario are about 44% lower than the CV scenario, and GHGs from the PHEV scenario are 5% lower than HEVs. For the two-segment case, the optimal solution is to allocate a PHEV40 to drivers who can charge every 87 miles or less (92% of drivers and 74% of vehicle miles traveled (VMT) per day) and allocate a smaller-range PHEV25 to drivers who charge less frequently. This optimal allocation of two vehicles reduces daily GHG emissions by only an additional 0.1% compared to allocating all drivers a PHEV36. The solution of three-segment case similarly produces small additional GHG reduction. A significant reduction in GHG emissions is achieved by allocating PHEVs to drivers rather than HEVs or CVs, and there is only a marginal additional gain from optimal allocation in the two- and three-segment cases.

Assigning all drivers high-AER PHEVs can significantly reduce petroleum consumption, but this is not necessarily the best solution for minimizing GHGs because reducing the number of underutilized batteries in these vehicles reduces the emissions associated with battery production as well as the emissions associated with reduced vehicle efficiency caused by carrying heavy batteries. While the largest group of vehicles travel short distances each day, the majority of the GHG emissions are produced by those vehicles that travel between about 25 and 45 miles/day. We further tested the single-segment case with a low carbon electricity mix scenario 218 kg-CO_2-eq/kWh [4]. The optimal solution shows a large-capacity PHEV87 (upper bound) is best to reduce GHG emissions to 4.53 kg-CO_2-eq per vehicle per day, 69% lower than CV and 45% lower than HEV.

To compare the solution performance of the randomized multistart method with global solutions, we use 1000 random starting points uniformly distributed in the design variable domain with the MATLAB SQP solver *fmincon* to minimize GHG solutions using Eq. (1) rather than Eq. (14). The integral in Eq. (1) is approximated by trapezoidal numerical integration, and each combination of vehicle type ordering (e.g., CV-PHEV, HEV-PHEV, etc.) is solved separately, so that the resulting formulation is a nonconvex NLP for each combination of vehicle types (the remaining derivative discontinuities in some of the functions were not observed to cause numerical problems when using finite difference methods). The solution quality is evaluated using relative error $|F-F^*|/F^*$, where F is the objective value found by the local solver in each

Table 2 Solutions of minimum lifecycle GHGs with three driver segment scenarios

	Single segment			Two segments		Three segments		
Driver segment scenario	CV	HEV	PHEV	PHEV	PHEV	PHEV	PHEV	PHEV
Allocation (miles)	0–200	0–200	0–200	0–87	87–200	0–33	33–83	83–200
AER (miles)	–	–	36	40	25	29	46	25
Engine power (kW)	126	57	46	47	43	44	49	43
Motor power (kW)	–	52	70	71	73	71	72	73
Battery cells	–	168	396	435	269	316	512	274
Battery design swing	–	–	0.8[a]	0.8[a]	0.8[a]	0.8[a]	0.8[a]	0.8[a]
Battery capacity (kWh)	–	1.3	8.6	9.4	5.8	6.8	11.0	5.9
CD-mode efficiency (miles/kWh)	–	–	5.30	5.29	5.35	5.33	5.25	5.34
CS-mode efficiency (mpg)	29.5	60.1	60.2	60.0	60.7	60.5	59.6	60.7
CD-mode acceleration (s)	–	–	11.0	11.0	11.0	11.0	11.0	11.0
CS-mode acceleration (s)	11.0	11.0	9.3	9.1	10.3	9.8	8.9	10.2
Final SOC	–	–	0.32	0.32	0.32	0.32	0.32	0.32
GHG emissions(kg-eq-CO_2 per vehicle-day)	14.6	8.2	7.78	7.77		7.75		
Reduction % from CV only	0%	−43.8%	−46.7%	−46.8%		−46.9%		

[a]Variable limited by model boundary.

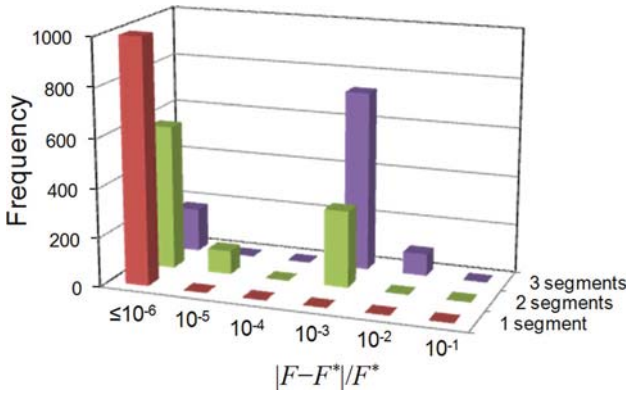

Fig. 2 Histogram for the solution errors of 1000 random multistarts with local NLP solver

multistart and F^* is the global solution. The results are presented in Fig. 2. All multistart points reached feasible solutions. For the single-segment model, and all multistart solutions reached the global optimum. For the two-segment case, 59% of the multistart solutions reach the global optimum within 10^{-6}. For the three-segment case, the global solution is found 18% of the time. At an 18% success rate, achieving 99.95% probability of finding the global minimum in each of ten sensitivity scenarios would require 50 randomized multistart runs per scenario. Using different NLP solvers or multistart randomization may affect the percentages, but results suggest that when the number of segments and decision variables increase, the probability of random starting points reaching global solution decreases. In this problem, local minima identified are all within 1% of the global minimum; however, variations of the problem could generate global minima of lower quality, and comparison across vehicle type cases and sensitivity cases could be affected if global solutions are not identified for every case.

4 Conclusions

We reformulate an optimization model to determine globally optimal vehicle design and allocation of conventional, hybrid, and plug-in hybrid vehicles to drivers in order to minimize life cycle GHG emissions. The reformulation is a twice-differentiable factorable algebraic nonconvex MINLP that can be solved globally using convexification with a branch-and-reduce algorithm implemented in GAMS/BARON. We find that minimum life cycle GHG emissions can be achieved with PHEVs sized for ~25–45 miles of electric travel. The results indicate that moving drivers from conventional vehicles to HEVs or PHEVs implies significant reductions in life cycle GHGs, but optimal allocation of different PHEV designs to different drivers is of second order importance. While larger battery packs may be better for reducing petroleum consumption, larger packs do not necessarily result in lower GHGs, and the best solution is a combination of midsized packs that reduce GHGs associated with production and weight of underutilized batteries. Grid decarbonization makes larger battery packs more competitive for GHG reduction.

Adoption of PHEVs will depend critically on cost. We examine cost and petroleum consumption objectives in a companion paper [5] and examine sensitivity of minimum cost and GHG solutions to variation in parameters such as battery prices, fuel and electricity prices, electricity grid mix, and carbon allowance prices. In comparing a randomized multistart approach to deterministic global optimization, we find that the probability of randomized multistart finding global solutions is relatively high for this problem, although it decreases as the number of segments and the number of sensitivity cases increase. The global MINLP framework presented here provides confidence in comparing solutions across sensitivity scenarios.

Acknowledgment

The authors would like to thank Professor Jay Whitacre, Professor Chris Hendrickson, Scott B. Peterson, and the members of the Design Decisions Laboratory, the Carnegie Mellon Green Design Institute and Vehicle Electrification Group for their feedback and help with model formulation. This research was supported in part by the National Science Foundation's CAREER Award No. 0747911, a grant from the National Science Foundation program for Material Use, Science, Engineering and Society (MUSES): Award No. 0628084, and grants from Ford Motor Company and Toyota Motor Corporation. C.-S.N. Shiau would like to acknowledge the support from the Liang Ji-Dian Fellowship.

References

[1] Bandivadekar, A., Bodek, K., Cheah, L., Evans, C., Groode, T., Heywood, J., Kasseris, E., Kromer, M., and Weiss, M., 2008, *On the Road in 2035: Reducing Transportation's Petroleum Consumption and GHG Emissions*, Massachusetts Institute of Technology, Cambridge, MA.

[2] Shiau, C.-S. N., Kaushal, N., Hendrickson, C. T., Peterson, S. B., Whitacre, J. F., and Michalek, J. J., 2010, "A Mixed-Integer Nonlinear Programming Model for Deterministic Global Optimization of Plug-In Hybrid Vehicle Design and Allocation," ASME 2010 International Design Engineering Technical Conferences, Montreal, Quebec, Canada.

[3] Frank, A. A., 2007, "Plug-In Hybrid Vehicles for a Sustainable Future," Am. Sci., **95**, pp. 158–165.

[4] Samaras, C., and Meisterling, K., 2008, "Life Cycle Assessment of Greenhouse Gas Emissions From Plug-In Hybrid Vehicles: Implications for Policy," Environ. Sci. Technol., **42**, pp. 3170–3176.

[5] Shiau, C.-S. N., Kaushal, N., Hendrickson, C. T., Peterson, S. B., Whitacre, J. F., and Michalek, J. J., 2010, "Optimal Plug-In Hybrid Electric Vehicle Design and Allocation for Minimum Life Cycle Cost, Petroleum Consumption, and Greenhouse Gas Emissions," ASME J. Mech. Des., **132**, p. 091013.
[6] Papalambros, P. Y., and Wilde, D. J., 2000, *Principles of Optimal Design: Modeling and Computation,* 2nd ed., Cambridge University Press, New York.
[7] Arora, J. S., Elwakeil, O. A., Chahande, A. I., and Hsieh, C. C., "1995, Global Optimization Methods for Engineering Applications—A Review," Struct. Optim., **9**, pp. 137–159.
[8] Conn, A. R., Scheinberg, K., and Vicente, L. N., 2009, *Introduction to Derivative-Free Optimization*, Society for Industrial and Applied Mathematics, Philadelphia, PA.
[9] Tawarmalani, M., and Sahinidis, N., 2002, *Convexification and Global Optimization in Continuous and Mixed-Integer Nonlinear Programming*, Kluwer Academic, Dordrecht, Netherlands.
[10] Federal Highway Administration, 2010, *National Household Travel Survey 2009*, Department of Transportation, Washington, DC.
[11] Tawarmalani, M., and Sahinidis, N.V., 2004, "Global Optimization of Mixed-Integer Nonlinear Programs: A Theoretical and Computational Study," Math. Programy., **99**, pp. 563–591.
[12] Grossmann, I., 2002, "Review of Nonlinear Mixed-Integer and Disjunctive Programming Techniques," Optim. Eng., **3**, pp. 227–252.
[13] Gunluk, O., and Linderoth, J., 2010, "Perspective Reformulations of Mixed Integer Nonlinear Programs With Indicator Variables," Math. Program., **124**, pp. 183–205.